creative commons
COMMONS DEED

저작자표시-비영리-변경금지 2.0 대한민국

이용자는 아래의 조건을 따르는 경우에 한하여 자유롭게

- 이 저작물을 복제, 배포, 전송, 전시, 공연 및 방송할 수 있습니다.

다음과 같은 조건을 따라야 합니다:

저작자표시. 귀하는 원저작자를 표시하여야 합니다.

비영리. 귀하는 이 저작물을 영리 목적으로 이용할 수 없습니다.

변경금지. 귀하는 이 저작물을 개작, 변형 또는 가공할 수 없습니다.

- 귀하는, 이 저작물의 재이용이나 배포의 경우, 이 저작물에 적용된 이용허락조건을 명확하게 나타내어야 합니다.
- 저작권자로부터 별도의 허가를 받으면 이러한 조건들은 적용되지 않습니다.

저작권법에 따른 이용자의 권리는 위의 내용에 의하여 영향을 받지 않습니다.

이것은 이용허락규약(Legal Code)을 이해하기 쉽게 요약한 것입니다.

Disclaimer

dCollection

교육학석사학위논문

Fluorescence-Raman Nanoprobes Synthesis for Fluorescence-Raman Endoscopic System and Its Application on Colorectal Cancer Model

형광-라만 동시 내시경을 위한 형광-라만 나노프로브 합성 및 직장암 모델에서의 활용에 관한 연구

2017 년 8 월

서울대학교 대학원

과학교육과 화학전공

이 성 균

Fluorescence-Raman Nanoprobes Synthesis for Fluorescence-Raman Endoscopic System and Its Application on Colorectal Cancer Model

지도교수 정 대 홍

이 논문을 교육학석사 학위논문으로 제출함

2017 년 8 월

서울대학교 대학원

과학교육과 화학전공

이 성 균

이민우의 교육학석사 학위논문을 인준함

2017 년 8 월

위 원 장 _____ (인)

부위원장 _____ (인)

위 원 _____ (인)

Abstract

Fluorescence-Raman Nanoprobes Synthesis for Fluorescence-Raman Endoscopic System and Its Application on Colorectal Cancer Model

Sung Gun Lee

Department of Science Education

(Major in Chemistry)

The Graduate School

Seoul National University

In recent years, endoscopic imaging techniques with the spectroscopic assistance have been actively developed due to both the increase in demand and necessity for

early diagnosis of cancer and the development of optical technology. These devices are classified into using intrinsic analysis methods that analyze signals based on living organs and using a labeling method that uses spectroscopic probes that specifically bind to specific biomarkers. Such techniques can be breakthrough for diagnosis of a lesion that has not been detected through white light endoscopic imaging technology. However, there are limits to the fluorescence-based markers currently being used. It have a wide bandwidth and possibility to overlap with auto-fluorescence emitted by tissue. To overcome these problems, recent studies suggest surface-enhanced Raman scattering (SERS) nanoparticles as alternative probes in molecular diagnosis. Raman signal have narrow bandwidth and high sensitivity that allows multiplexed diagnosis in endoscopic methods.

In this study, we synthesized optically stable fluorescence-SERS nanoprobes (F-SERS dot) that have separated fluorescence from Raman signal without interference. In order to utilize the F-SERS dots as nanoprobes for cancer-specific biomarkers, the antibodies were immobilized on the particle surface by EDC/NHS coupling method. To confirm the specificity of the synthesized F-SERS dots, epidermal growth factor receptor (EGFR) and vascular endothelial growth factor (VEGF) were selected as tumor cell biomarkers in colorectal cancer mouse model. We conjugated antibodies which specifically binding with each antigen type with different Raman molecule labeled F-SERS dot, then we confirmed the feasibility of F-SERS dots at *in vitro* and *in vivo* diagnosis of colorectal cancer model.

Key words: Fluorescence-Raman Nanoprobe (F-SERS dot), Surface-Enhanced Raman Scattering (SERS), Fluorescence-Raman Endoscopic System, In Vivo Multiplexed Molecular Diagnostics

Student number: 2015-23061

Contents

List of Figure

1. Introduction

The endoscopy based diagnostics are the most common and essential diagnostic tool in modern medicine. In wide-field white-light endoscopic system, it visualizes the surface morphology in hollow organs and it contributes on early detection of cancer. Despite the development of imaging technology such as increased imaging resolution or narrow band imaging (NBI), there were not dramatic advancement in diagnostic accuracy based on wide-field endoscopy[1-3]. Because current wide-field endoscopic system only provides the morphological information rather than abnormality information of tumor suspected lesion. Consequently, there are limitations to find flat lesion at the early-stage neoplasia in endoscopic imaging technics[4-5].

To overcome the problem in common endoscopy, there have been attempts to integrate of molecular imaging tool, such as fluorescence, Raman, radioisotope probe[6-12]. Among these techniques, fluorescence assisted endoscopy is an intraoperative molecular diagnostic method that have widely applied on medical field. The principle of fluorescence probe based endoscopy resemble fluorescence guided surgery system in principle. For example, fluorescence labeled antibody or affinity peptide were sprayed on tumor suspected area and excitation source combined endoscopy probes were attached to lesion to detect the fluorescence signals from fluorescence stained dysplasia[13-14].

As another biophotonic tool, researchers considered Raman spectroscopy in order to enhance the accuracy of the diagnosis on endoscopic system[15-17]. In early development step of Raman aided endoscopy, there were attempts to investigate the Raman signals as fingerprints of tumor or precancerous lesion. Riccardo et al. used Raman spectroscopic endoscope for diagnosis of melanocytic lesion from normal tissue by detecting the Raman shift with Amide I and Amide III concentration changes[18]. However, these kind of intrinsic Raman signal based endoscopy have limitation, they do not provide distinctive spectral change at normal and cancerous tissue. As a result, intrinsic Raman endoscopy rely on clinical big data that collected from long-term studies of patients, and have high false-positive/negative results[19].

As an alternative to intrinsic Raman, Raman tagging agents based on nanoprobes were proposed. Because of dramatically enhanced Raman signal in vicinity of the noble metal surface up to 10-14 orders of magnitude that called surface-enhanced Raman scattering (SERS), it compensates for the low sensitivity of the Raman signals and provides unique spectral fingerprints for tagging the biomarkers at *in vivo* diagnosis[20,21]. In addition to high sensitivity, SERS have more multiplexing capability than another labeling method. In contemporary manner of the multiplexed labeling can be achieved by combination of fluorescence dye which has high sensitivity, but fluorescence has relatively broad emission bandwidth that leads to overlap of peaks. It restricts multiplexing capacity by fluorescence molecule[22]. On the other hand, SERS labeled nanoprobes give relatively narrow bandwidth that

enable multiplexed labeling in diagnosis level[23]. In this perspective, fluorescence and Raman dual modal nanoprobes can achieve high sensitivity and large multiplexing capability with real-time acquisition in endoscopic system.

In this research, we validated the feasibility of fluorescence-Raman active nanoprobes (F-SERS dots) on fluorescence-Raman dual modal endoscopic system (FRES) which can detect fluorescence and Raman signals simultaneously by single excitation source. To attain this end, we synthesized F-SERS dots that emits fluorescence and Raman signal with separated window at the same time, and evaluated the possibility of F-SERS dots in FRES. After validating F-SERS dots signal, then we utilized the F-SERS dots on colorectal cancer *in vitro* cell model and *in vivo* mouse model.

2. Experimental Section

2.1 Chemicals and Materials Tetraethyl orthosilicate (TEOS), ammonium hydroxide (NH_4OH, 28-30%), 3-mercaptopropyltrimethoxysilane (MPTS), silver nitrate ($AgNO_3$, > 99.99%), ethylene glycol (EG, spectrometric grade, > 99%), octylamine (OA), rhodamine B isothiocyanate (RBITC), fluorescein isothiocyanate (FITC), sodium silicate, 3-aminopropyltriethoxysilane (APTES), succinic anhydride, *N,N'*-diisopropylethylamine (DIEA), *N*-hydroxysuccinimide (NHS), dimethylaminopyridine (DMAP), *N,N'*-diisopropylcarbodiimide (DIC), Phosphate buffered saline tablet and bovine serum albumin (BSA, > 98%) were purchased from Sigma-Aldrich (St. Louis, MO, USA). Zoletil 50 (tiletamine-zolazepam) was purchased from Virbac S.A. (Carros, France). Xylazine (Rompun) was purchased from Bayer (Leverkusen, Germany). Alexa Fluor 610 dye conjugated succinimidyl ester was purchased from Invitrogen (Carlsbad, CA, USA). Cetuximab (anti-epidermal growth factor receptor (anti-EGFR) monoclonal antibody) and Bevacizumab (anti-vascular endothelial growth factor (anti-VEGF) monoclonal antibody) were purchased from Merck Millipore (Darmstadt, Germany). Isotype controlled mouse IgG was purchased from Abcam (Cambridge, United Kingdom). Absolute ethanol (99.9%), anhydrous ethanol (99%), 2-propanol (99%) were purchased from Daejung Chemicals (Siheung, Korea). Paraformaldehyde was purchased from Wako (Osaka, Japan) All chemicals were used without further purification. 8-well chambered coverglass was purchased from Lab-Tek (New York,

USA).

2.2 Synthesis of fluorescence-Raman dual modal nanoprobes (F-SERS dots)

The silica nanoparticles (SiNPs) of *ca* 180 nm diameter were synthesized by the Stöber method[24]. 1.6 mL of Tetraethyl orthosilicate (TEOS) was dissolved in 40 mL of absolute ethanol and a 4.0 mL of NH_4OH (28-30%) was added to the mixture. The mixture was vigorously stirred for 20 h at 25 °C. The synthesized SiNPs were centrifuged and washed with ethanol several times for purification. Then, 100 mg of SiNPs were dispersed in 2 mL of ethanol and 100 μL of MPTS and 20 μL of NH_4OH (28-30%) added to the mixture for functionalization of thiol group on the surface of the SiNPs. This mixture was vigorously stirred for 12 h at 25 °C, and subsequently the thiol functionalized SiNPs solution was centrifuged and re-dispersed in ethanol for several times. In order to introduce silver nanoparticles onto the SiNP surface, 100 mg of thiol-treated SiNPs were dispersed in 25 mL of ethylene glycol and were mixed with 25 mL of silver nitrate solution (6 mM in ethylene glycol). 41.24 μL of Octylamine (5mM) was added to the mixture and stirred for 1 h as the mild reducing agent and capping agent. In order to encode Raman-labeling compounds, silver-embedded silica nanoparticles were treated with 1 mM RBITC or 1 mM FITC, respectively. The Raman labeled silver embedded silica nanoparticle were then encapsulated with a silica shells using TEOS and NH_4OH. Further encapsulation

with fluorescent dye (AF 610)-conjugated silica shells was performed in a 10 μL of TEOS, 0.5 mL of NH_4OH (28-30%), and 55 μL of AF610-3-aminopropyltriethoxysilane (APTES) conjugated solution previously prepared by reacting 5 μL AF610 (8 mM in dimethyl sulfoxide (DMSO)) with 50 μL APTES (19.2 mM in ethanol) for 15 h. The final synthesized nanoprobes ($F\text{-}SERS_{RBITC}$ and $F\text{-}SERS_{FITC}$ dots) were washed with ethanol several times for purification and then dispersed in ethanol.

2.3 Antibody immobilization on the F-SERS dots. 1 mg of the F-SERS dots were dissolved in 1 mL of the APTES solution (5% in ethanol), and 10 μL of NH_4OH (28-30%) was added to the solution. Then, the solutions were vigorously stirred for 1 h at 50 °C for functionalization of amino group on the surface. The amine-functionalized F-SERS dots were washed with ethanol several times for purification and then re-dispersed in 0.5 mL of NMP. After functionalization of amino groups on F-SERS dots, we introduced carboxyl groups by adding 1.75 mg of Succinic anhydride and 3.05 μL of DIEA to the F-SERS dots solution. The mixture was stirred for 2 h at room temperature. Subsequently, the carboxyl -functionalized F-SERS dots were washed with NMP several times for removing excess reagents. Then, 54 μL of DIC, 40 mg of NHS, and 2.1 mg of DMAP were added to the carboxyl -functionalized F-SERS dots solution to activate the carboxyl groups for antibody conjugation. The resulting mixture was stirred for 2 h and then washed

with PBS three times. 50 mg of Cetuximab (Anti-EGFR monoclonal antibody) or 50 mg of Bevacizumab (Anti-VEGF monoclonal antibody) was added to the NHS-activated F-$SERS_{RITC}$ dots, F-$SERS_{FITC}$ dots dispersed in 200 mL of PBS. The mixture was incubated for 1 h at room temperature. The antibody-immobilized F-SERS dots were centrifuged and washed with PBS containing Tween 20 (0.2%), consecutively. Finally, the antibody-immobilized F-SERS dots were treated with BSA (1% in PBS solution) for 30 minutes and washed with PBS solution three times.

2.4 Orthotopic colorectal cancer (CRC) xenografts. All animal protocols were approved by the Institutional Animal Care and Use Committee of the Seoul National University College of Medicine, and all experiments were performed in accordance with relevant guidelines and regulations. Six-week-old male BALB/c nude mice were obtained from Orient Bio, Inc. (Seoul, Korea) and housed in a specific, pathogen-free environment. 1×10^7 of HT29-effluc cells injected for antibody blocking study in FRES imaging.

Before each injection of tumor cells, mice were anesthetized with an intramuscular injection of 200 μL of zoletil 50 (0.5%) and xylazine (0.2%) solution (1:1). Using a 30-gauge needle, a 0.1 mL volume of complex (containing tumor cells at a 1:1 ratio in medium/matrigel) was injected into the posterior colorectal wall via the anus49, 50. Tumor growth was investigated over two weeks for the injection of 1×10^7 of HT29-effluc cells groups, and over one week for the injection of 5×10^6 of

HT29-effluc cells group.

2.5 *In vitro* validation of FRES measurements. Different density of HT-29 effluc cells (0, 10^3, 10^4, and 10^5 cells/cm^2) were seeded in an 8-well chambered coverglass with 300 μL of cell media per well. After 24 h incubation at 37 °C, cells were fixed with 4% paraformaldehyde for 20 min, and washed three times with PBS. 10 μg of F-SERS$_{RBITC/EGFR}$ dots in PBS solution containing 1% BSA were added to each well, incubated at room temperature for 10 min, washed three times with PBS, and FRES imaging was performed for 3 min.

2.6 Blocking study of FRES using cold antibodies. After two weeks of injecting 1× 10^7 HT29-effluc cells orthotopically, a blocking study was carried out using cold antibodies (anti-EGFR and/or anti-VEGF) for 10 min. After blocking, 100 μg of antibody-conjugated F-SERS dots (F-SERS$_{RBITC/EGFR}$ dot and F-SERS$_{FITC/VEGF}$ dot) were sprayed onto the tumors, which were then investigated using a FRES probe after 10 min of incubation and PBS washing.

2.7 Characterization and measurement UV-visible extinction spectra of F-SERS dots were measured by using UV-visible spectrometer (Cary 300, Varian, USA). The size and morphology of the F-SERS dots were characterized by using a TEM instrument (JEM1010, JEOL). Fluorescence and Raman signals of F-SERS

dots were measured using a confocal-microscope Raman system (LabRam 300, JY-Horiba, France) equipped with an optical microscope (BX41, Olympus, Japan). In this confocal Raman system, the fluorescence and Raman signals were collected in a back scattering geometry and detected by a spectrometer equipped with a thermos-electrically cooled (-70 °C) CCD detector (iDus DU420, Andor, UK). The 532 nm line of a diode-pumped solid laser (Samba™, Cobolt, Sweden) was used as an excitation source. Focusing of the excitation light source and collection of the Raman signals were accomplished by the same 100X objective lens (NA 0.90, Olympus, Japan). The strong Raylegh-scattering light was eliminated by a 532 nm long-pass edge filter. Both Raman signals were acquired using 3.6 mW laser power and 1 s acquisition time.

FRES consist of internal laser scanning module and external spectrum separation system. A custom-made type of confocal laser endoscope system (Cellvizio, Mauna Kea, France) were used as internal dual-axis laser scanning module. It combined with optical fiber bundle (Ultraminio, Mauna Kea, France) which delivered laser light to sample and collected fluorescence and Raman signals. The fluorescence and Raman signal that collected by fiber bundle probe, were delivered by another fiber and it carried signals to external wavelength separation system. External separation system consists of a long-pass filter (585 nm bright line single edge dichroic beamsplitter, Semrock, US) and an edge filter (532 nm Razoredge long wave pass filer, Semrock, US). The 585 long pass filter separated scattering light with

fluorescence light from F-SERS dots, and the 532 nm edge filter separated Raman scattering (Stokes scattering) with Rayleigh scattering. The separated Raman signal were detected by a spectrometer (SE 303i-A, Andor, UK) with a thermos-electrically cooled CCD detector (iDus DV401, Andor UK) was utilized. The fluorescence image was delivered into scanning unit and collected by an avalanche photodiode and processed into real-time images (12 fps) by the imaging program (ImageCell, Mauna Kea, France). An excitation source of this system used a diode-pumped solid state laser (Samba^{TM}, Cobolt, Sweden) coupled with a single mode fiber.

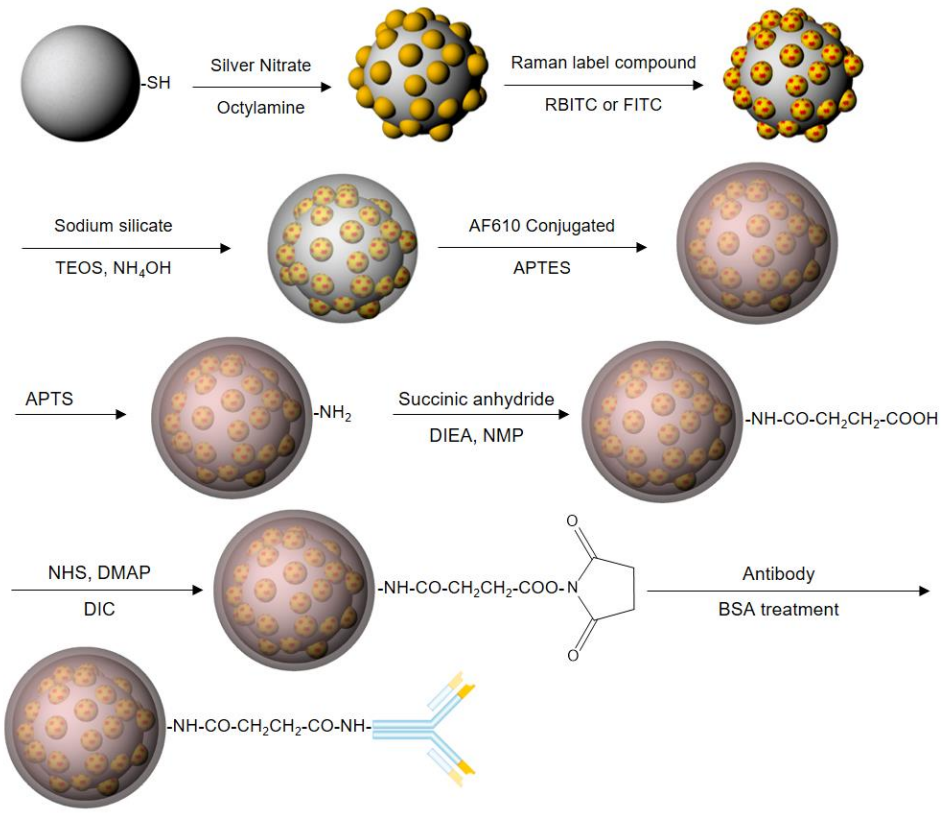

Figure 1. Schematic illustration of overall fabrication process of antibody conjugated F-SERS dot.

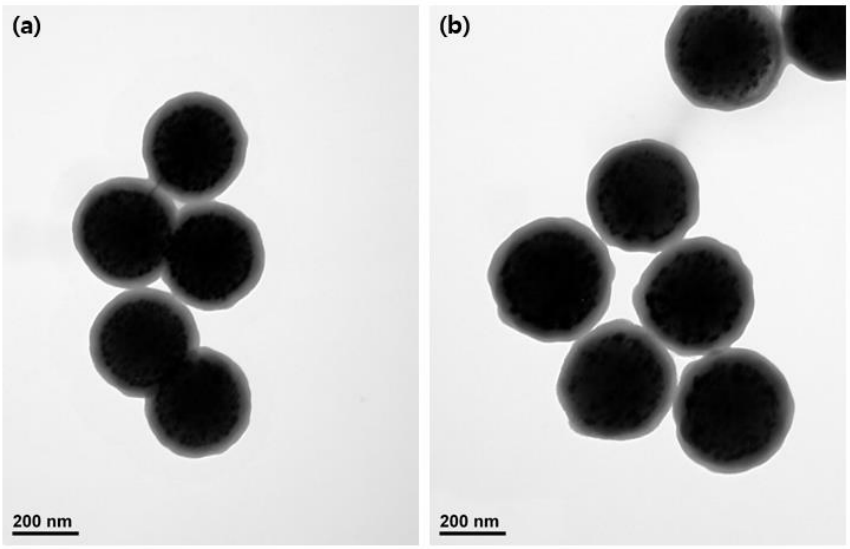

Figure 2. Transmission electron microscopy (TEM) image of (a) F-$SERS_{RBITC}$ dot (b) F-$SERS_{FITC}$ dot. (c) UV-Visible extinction spectra of F-$SERS_{RBITC}$ and F-$SERS_{FITC}$ dot.

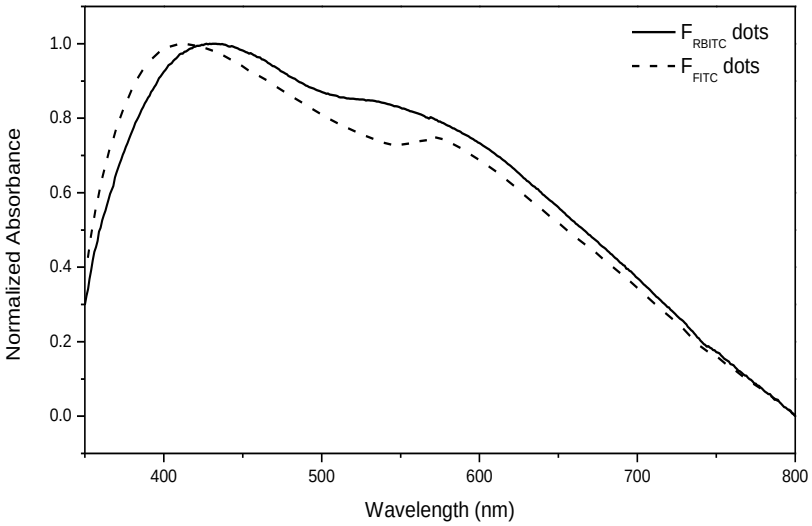

Figure 3. UV-Visible extinction spectra of F-SERS$_{RBITC}$ (straight line) and F-SERS$_{FITC}$ (dashed line) dot.

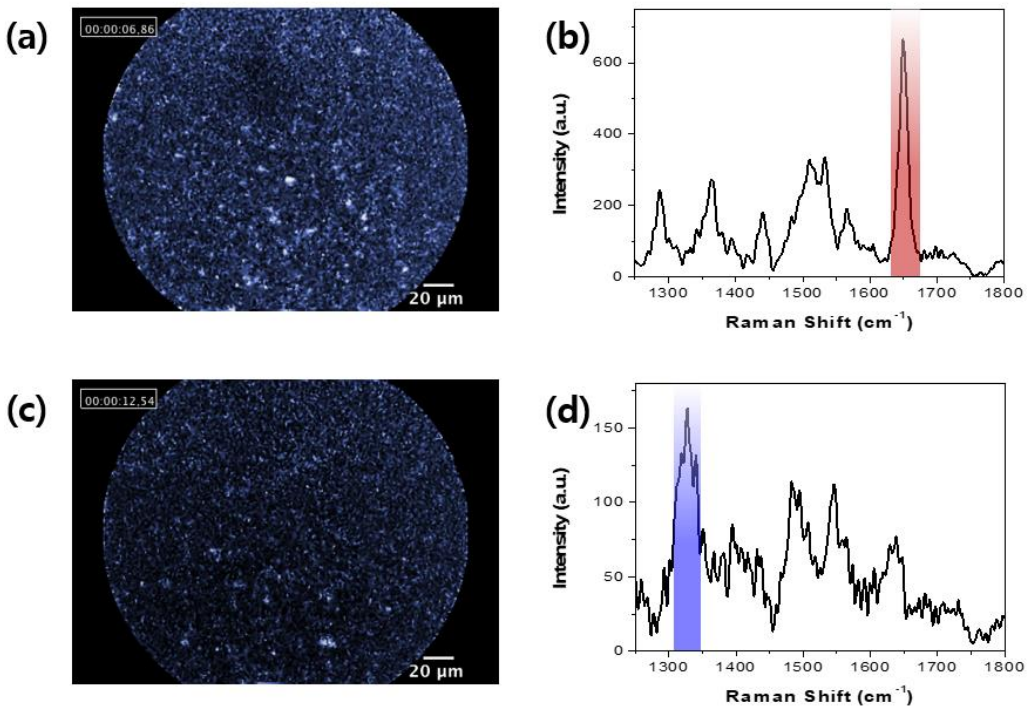

Figure 4. (a) Fluorescence images and (b) Raman spectra of F-SERS$_{RBITC}$ dot. (c) Fluorescence images and (d) F-SERS$_{FITC}$ dot. All images acquired using FRES at laser power of 2.7 mW. The SERS spectra were obtained for 1 s. All fluorescence images are fake colored.

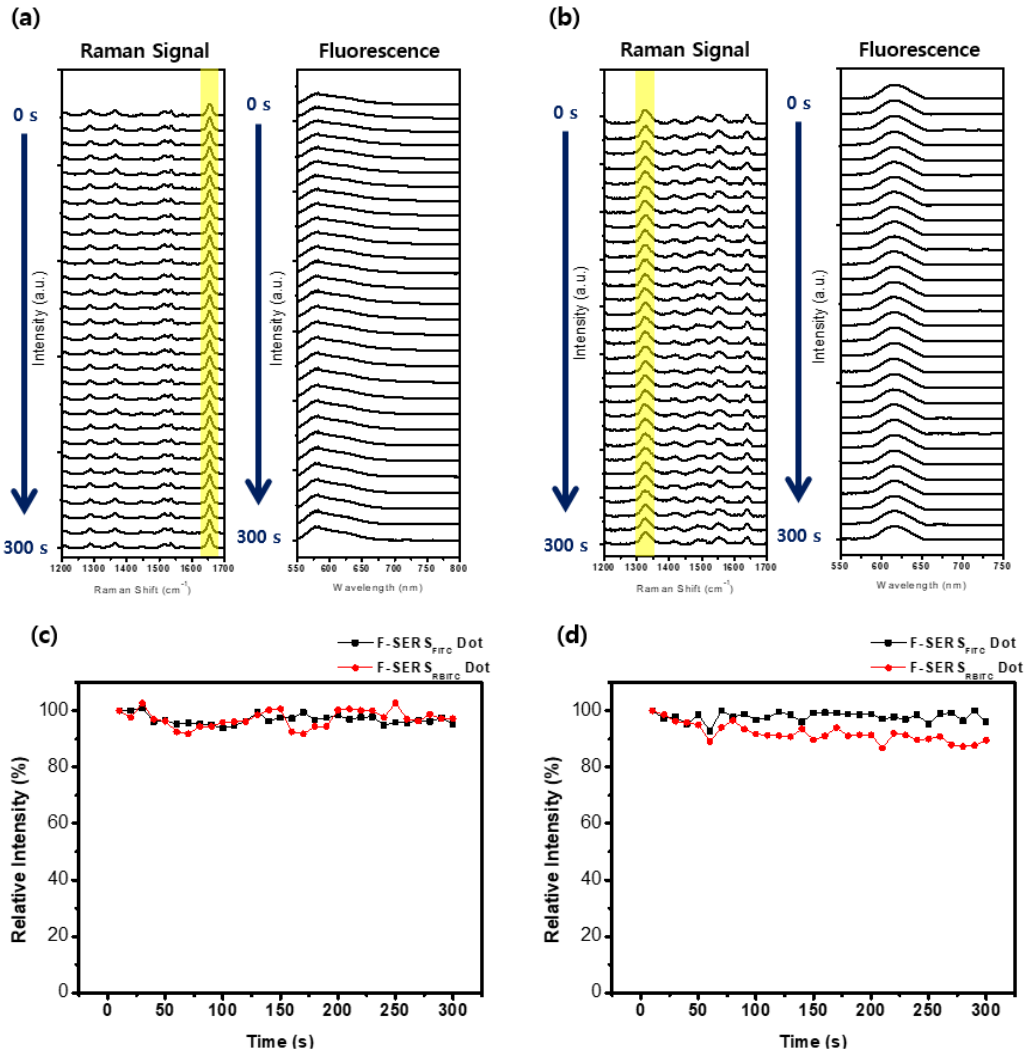

Figure 5. Photostability test of single F-SERS dot for 300 s. Individual and Raman spectra of (a) F-SERS$_{RBITC}$ dot (b) F-SERS$_{FITC}$ with 532 nm laser excitation (3.6 mW, 1 s acquisition). (c) Fluorescence intensity at 625 nm and (d) Raman intensity (at 1648 cm^{-1} for RBITC and 1324 cm^{-1} for FITC) with 532 nm laser excitation (3.6 mW, 1 s acquisition).

3. Results and Discussion

3.1. Synthesis and characterization of fluorescence Raman dual modal nanoprobes(F-SERS dots)

Fluorescence-Raman dual modal nanoprobe (F-SERS dot) emits fluorescence and SERS signal simultaneously but it was designed to emit the signals with different wavelength position. It is considered to avoid the intrinsic Raman scattering of the fiber bundle probe of the FRES. The optical noise of the FRES probe is intensive below 1000 cm^{-1} and their intensity is about 10^2 larger than SERS signal of the F-SERS dot. Therefore, RBITC/FITC were introduced as Raman label compounds which have individually distinguishable Raman peak over the 1000 cm^{-1} area (1648 cm^{-1} for F-$SERS_{RBITC}$ dot and 1324 cm-1 for F-$SERS_{FITC}$ dot). In addition to the isolation Raman peaks from intrinsic noise of fiber bundle, fluorescence signal should be separated from Raman signal. In FRES instrument, a 532 nm laser used as an excitation source for simultaneous acquisition of fluorescence and Raman signal. In this excitation condition, the distinguishable Raman signals of F-$SERS_{RBITC/FITC}$ dots are on ~580 nm, thus the spectral window for the fluorescence signal acquisition should be over 600 nm. In order to introduce the fluorescence dye on the Raman labeled nanoprobe ($SERS_{RBITC/FITC}$ dot), Alex flour 610 dye conjugated with APTES and subsequently the dye conjugated APTES was added to SERS dot to introduce outer fluorescence silica shell by silanization. As shown in Figure 2, overall diameter of the F-SERS dots is *ca.* 230 nm and their extinction spectra has

broad range over visible area. It can be interpreted as the plasmonic coupling of the introduced silver nanoparticles on the surface of the silica nanoparticle.

To evaluate the dual modality of the F-SERS dots, each F-SERS dots were dispersed to 1% BSA solution in micro tube, and simultaneously measured the fluorescence and Raman signals by FRES. In figure 4 a and c, fluorescence of each F-SERS dots was distinguishable from the dark blue background as a bright dot in fluorescence image. In figure 4 b and d, specific band of each F-SERS dots was could be identified with different band position: 1648 cm^{-1} band for $F\text{-}SERS_{RBITC}$ dots and 1324 cm^{-1} band for $F\text{-}SERS_{FITC}$ dots. Synthesized F-SERS dots were stabled under laser irradiated condition. As shown in figure 5, fluorescence of the F-SERS dots were not decreased by 3.6 mW of 532 nm laser irradiation for 300 s, and Raman signals of $F\text{-}SERS_{RBITC}$ dots were slightly decreased (10% for 300 s) that doesn't cause meaningful photobleach. These results indicate that the F-SERS dots could be used as *in vivo* tracking nanoprobes in FRES examination.

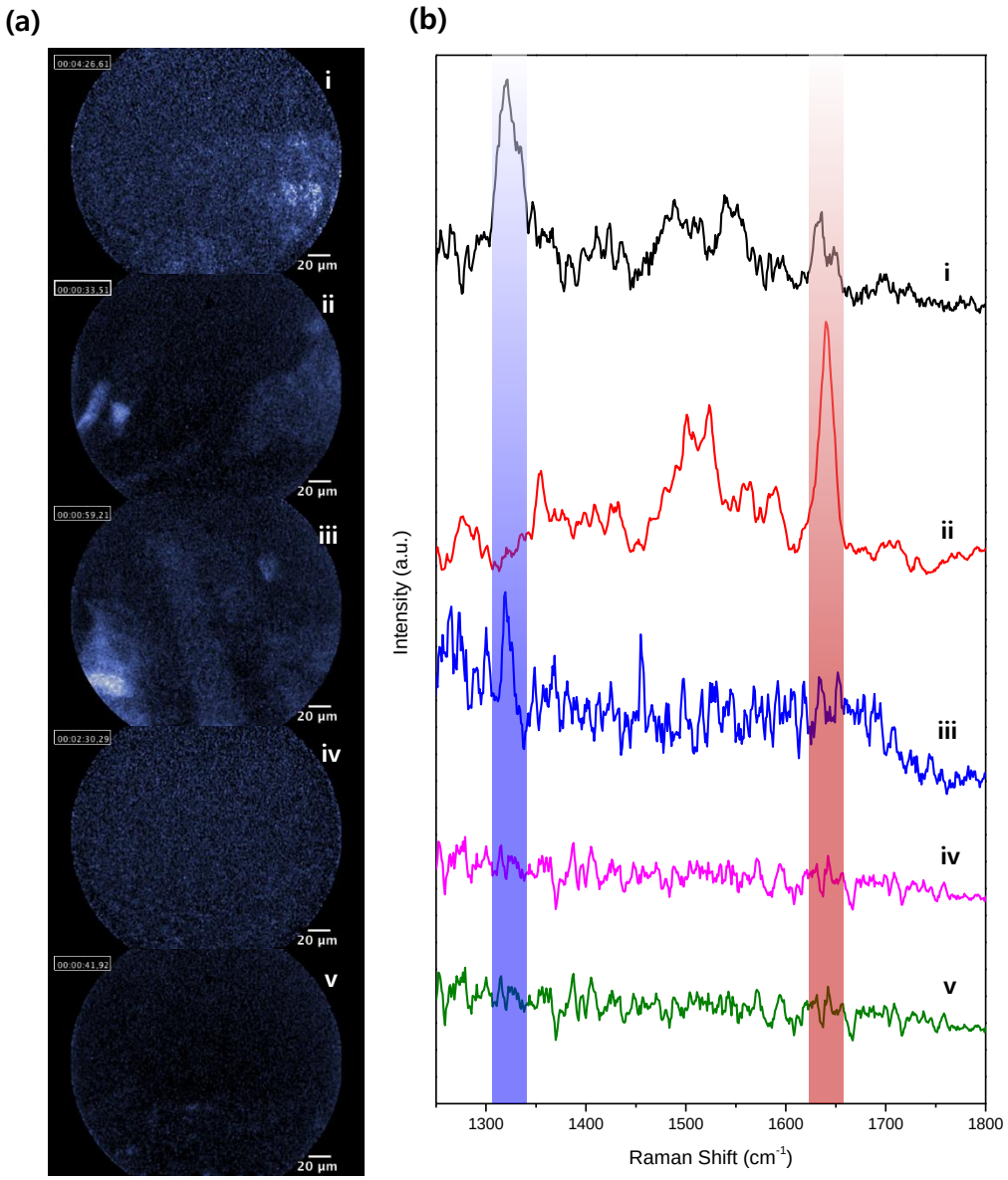
(a)
(b)
00:04:26.61
i
20 μm
00:00:33.51
ii
20 μm
00:00:59.21
iii
20 μm
00:02:30.29
iv
20 μm
00:00:41.92
v
20 μm
Intensity (a.u.)
1300
1400
1500
1600
1700
1800
Raman Shift (cm-1)
i
ii
iii
iv
v

Figure 6. *in vivo* diagnosis of tumor by FRES. After 2 weeks of injecting HT29-effluc cells, tumor lesion of each mice model was treated different antibody mixture. (a) AF610 fluorescence image was obtained for real time (12 frames/s) and (b) Raman spectra is acquired for 1 s. Both fluorescence and Raman signal were obtained by 532 nm laser with 2.7 mW. Each tumor lesion (i), (v) not blocked by antibody, (ii) blocked by anti-VEGF antibody, (iii) blocked by anti-EGFR antibody, (iv) blocked by anti-EGFR and anti-VEGF antibody. After antibody blocking, the tumor lesion in (i)~(iv) was treated by 10 μg of F-SERS$_{RBITC/EGFR}$ dots and 10 μg of F-SERS$_{FITC/VEGF}$ dots. (v) was treated by 10 μg of F-SERS$_{RBITC/IgG}$ dots as a control group.

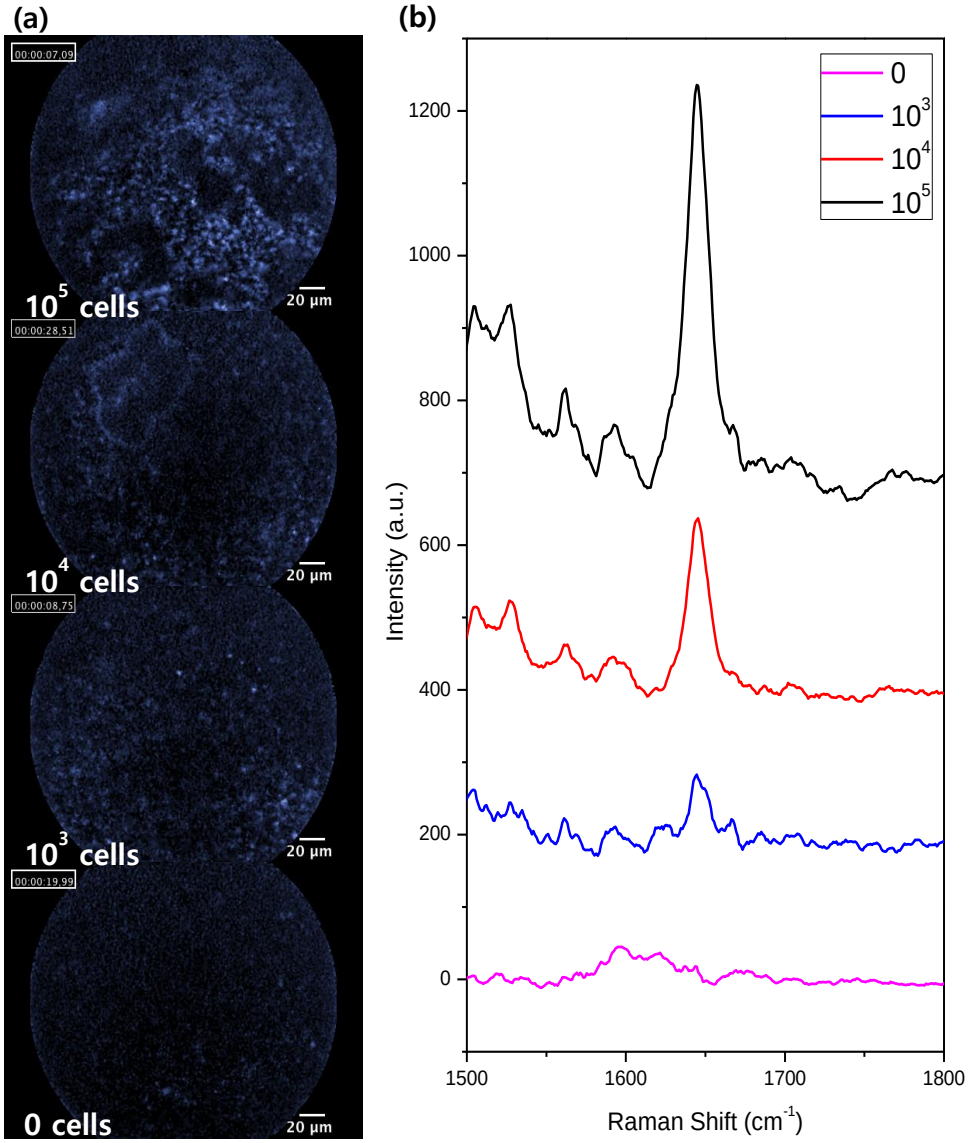
(a)
00:00:07,09
10^5 cells
20 μm
00:00:28,51
10^4 cells
20 μm
00:00:08,75
10^3 cells
20 μm
00:00:19,99
0 cells
20 μm
(b)
0
10^3
10^4
10^5
Intensity (a.u.)
0
200
400
600
800
1000
1200
1500
1600
1700
1800
Raman Shift (cm^-1)

Figure 7. *in vitro* FRES test on seeded cells on well plate. F-$SERS_{RBITC/EGFR}$ dots were used to detect the HT29-effluc cells. Fluorescence signal (a) and Raman intensity at 1648 cm^{-1} (b) gradually become definite as the cell number increases.

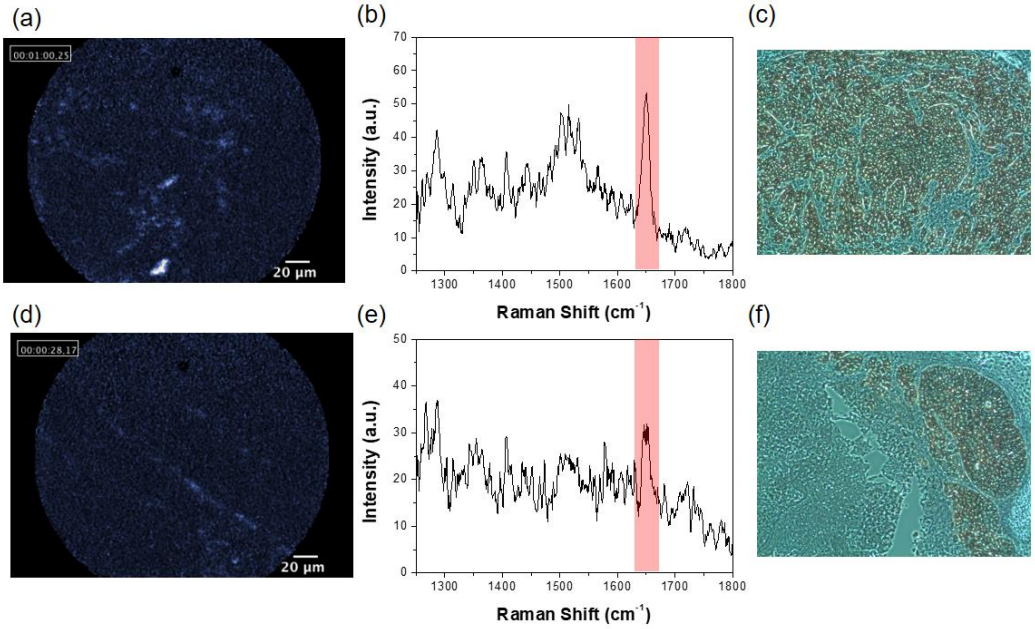

Figure 8. Detection of heterogeneous EGFR expression by FRES *ex vivo*. 100 μg of F-SERSRBITC/EGFR dots sprayed onto tumors and tissues were investigated using FRES. Fluorescence imaging acquired by AF610 fluorescence dye (a)(d), and Raman intensity showed at 1648 cm^{-1} (b)(e) . EGFIR expression with IHC (c)(f) were different in two samples.

3.2. Application of the F-SERS dots on FRES colorectal cancer diagnosis

To applicate F-SERS dots on FRES for noninvasive *in vivo* multiplexed diagnostics, active targeting experiment performed at colorectal cancer cells (HT29) xenograft model. The characterization of colorectal cancer is necessary for the decision of appropriate treatment option. In standard therapy, Cetuximab (anti-EGFR monoclonal antibody) and Bevacizumab (anti-VEGF monoclonal antibody) were used as targeted therapy for colorectal cancer. In these backgrounds, EGFR and VEGF were selected as targets in this study. Each mice distributed for four groups (i) tumor treated with PBS (ii) tumor treated with 100 μg of anti-VEGF cold antibody (iii) tumor treated with 100 μg of anti-EGFR cold antibody (iv) tumor treated with 50 μg of anti-EGFR and 50 μg of anti-VEGF cold antibody for dual blocking. After cold antibody blocking treatment, 100 μg of antibody conjugated F-SERS dots (mixture of F-SERS$_{RBITC/EGFR}$ dots and F-SERS$_{FITC/VEGF}$ dots) were sprayed over tumor lesion and washed out. Tumors without blocking treatment showed both fluorescence and Raman signals of RBITC and FITC (Figure 6a-i, 6b-i). Single antibody blocking treated tumors with anti-VEGF antibody (Figure 6a-ii, 6b-ii) were showed fluorescence and Raman signal by EGFR active F-SERS$_{RBITC}$ dots, on the other hand anti-EGFR antibody (Figure 6a-iii, 6b-iii) were showed fluorescence and Raman by VEGF active F-SERS$_{FITC}$ dots. Dual antibody blocking treated tumors revealed only auto-fluorescence but no significant fluorescence and Raman signals. After validated the feasibility of F-SERS dots on FRES system,

mouse IgG active F-$SERS_{RBITC}$ dots were synthesized as a control group. F-$SERS_{RBITC/IgG}$ dot were sprayed on tumor lesion which blocked by neither EGFR nor VEGF antibody. It revealed no relevant Raman and fluorescence signals on tumor area, which showed F-$SERS_{RBITC/IgG}$ dots were not actively targeted on the tumor site. It could be understood that there was no detectable nonspecific binding *in vivo* model, and there are not meaningful cross-contamination possibility on multiplexed-diagnosis. If there were detectable nonspecific bindings *in vivo* model, qualitative and quantitative analysis of antigens could not be achieve in this manner, but this result showed that there are not distinguishable possibility of nonspecific bindings.

After validating the feasibility of F-SERS dots on colorectal cancer mouse model *in vivo*, we attempted to evaluate the relative quantification ability of F-SERS dots *in vitro* and *ex vivo*. HT29-effluic cells were cultured on well plated glass with 0, 10^3, 10^4, 10^5 cells/cm^2 density. Then, each well was filled with 10 μg of F-$SERS_{RBITC/EGFR}$ dots solution. After incubation and careful washing process, FRES probe were attached to cell area and fluorescence and Raman signals were acquired. Fluorescence image was gradually brighten as the cell density increases, also Raman signal intensity from RBITC were increased: 100 counts (10^5 cells/cm^2), 40 counts (10^4 cells/cm^2), 25 counts (10^3 cells/cm^2), and there were no significant signals without cultured cells. However, in vitro model assume the ideal model for tumor lesion which is made of only tumor cells, but in vivo tumor model has heterogeneity in expression of the tumor marker that gives the information of the progression and

condition of cancer. Therefore, it is important to validate the relative quantitative analysis of F-SERS dots on heterogeneous tumor *ex vivo* model.

For the evaluation of F-SERS dots on *ex vivo* model, HT-29 cells were injected to the mouse. After 1 week of injection, tumors were excised and divided into halves. One half was targeted by F-SERS$_{RBITC/EGFR}$ dots and tested by FRES and the other was examined by IHC. As shown in figure 8, highly EGFR expressed tumor area gave relatively bright real-time fluorescence image and high Raman intensity (Raman intensity of 45 count). On the other hand, regularly EGFR expressed tumor gave low fluorescence and Raman signals (Raman intensity of 20 count).

These *in vitro* and *ex vivo* results indicate F-SERS dots can be useful staining agents for not only qualitative tumor diagnosis but relatively quantitative analysis on antigen expression examination that indicate the condition of lesion presumed to be cancer.

4. Conclusion

In this study, fluorescence-Raman nanoprobes (F-SERS dots) applied on multiplexed diagnostic agent by fluorescence-Raman endoscopic system (FRES). The F-SERS dots were designed to simultaneously emit fluorescence and SERS signals at separated spectral window with single excitation source. Thus the fluorescence signals were used as imaging tools which can help to find the area of targeted nanoprobes and Raman signals were used for identifying the targeted nanoprobes.

To evaluate the feasibility of the F-SERS dots on FRES we demonstrate *in vitro* and *in vivo* experiments on colorectal cancer model. We cultured EGFR expressed cell lines on well plates with different density, then it was confirmed that the fluorescence and SERS intensity were increased by increasing tumor cell density on the well. After *in vitro* cancer cell detection, we demonstrated multiplexed diagnostics on colorectal cancer xenografted mouse model. The colorectal cancer was tracked by EGFR or VEGF markers specific antibody-bind F-SERS dots. To examine the multiplexing possibility of F-SERS$_{RBITC/EGFR}$ dots and F-SERS$_{FITC/VEGF}$ dots, we treated cold antibodies on cancer lesion for blocking specific antigens. Each F-SERS dots were only specifically bind on non-blocked antigens.

Thus, the results from this study was evaluated the feasibility of F-SERS dots on FRES device and they have potential to apply on multiplexed diagnosis based on endoscope.

5. References

1. Maximilian J. W. et al. Confocal laser endomicroscopy and narrow-band imaging-aided endoscopy for *in vivo* imaging of colitis and colon cancer in mice. *Nat. Protoc.* **6**, 1471-1481 (2011).
2. Fabian E. et al. Narrow-band imaging optical chromocolonoscopy; Advantages and limitations. *World J. Gastroentero*. **14**(31), 4867-4872 (2008).
3. Timothy J. M. et al. Evaluation of quantitative image analysis criteria for the high-resolution microendoscopic detection of neoplasia in Barrett's esophagus. *J. Biomed. Opt.* **15**(2), 026027 (2010).
4. David F. B. et al. The Clinical Consequences of Advanced Imaging Techniques in Barrett's Esophagus. *Gastroenterology*. **146**(3), 622-629 (2014).
5. Crow P. et al. Assessment of fiberoptic near-infrared Raman spectroscopy for diagnosis of bladder and prostate cancer. *Urology.* **65**, 1126-1130 (2005).
6. Boerwinkel D. F. et al. Endoscopic tri-Modal imaging and biomarkers for neoplasia conjoined: a feasibility study in Barrett's esophagus. *Dis. Esophagus*. **27**. 435-443 (2014).
7. Obrad R. et al. A multimodal spectroscopy system for real-time disease diagnosis, *Rev. Sci. Instrum.* **80**(4), 043103 (2009).

8. Garai, E. et al. High-sensitivity, real-time, ratiometric imaging of surface-enhanced Raman scattering nanoparticles with a clinically translatable Raman endoscope device. *J. Biomed. Opt.* **18**, 096008 (2013).
9. Supang K. et al. Progress in molecular imaging in endoscopy and endomicroscopy for cancer imaging, *J. Healthc. Eng*. **4**(1), 1-22 (2012).
10. Andreas S. et al. An unmet medical need: advances in endoscopic imaging of colorectal neoplasia. *J. Biophotonics*. **4**, 482-489 (2011).
11. Chen Y. et al. Gold nanocages as contrast agents for two-photon luminescence endomicroscopy imaging. *Nanomedicine.* **8**, 1267-1270 (2012).
12. Lee H. et al. An Endoscope with integrated transparent bioelectronics and theranostic nanoparticles for colon cancer treatment. *Nature.* **6**, 10059 (2015).
13. Atreya, R. et al. *In vivo* imaging using fluorescent antibodies to tumor necrosis factor predicts therapeutic response in Crohn's disease. *Nat. Med*. **20**, 313-318 (2014).
14. Ying P. et al. Endoscopic molecular imaging of human bladder cancer using a CD 47 antibody. *Sci. Transl. Med*. **6**(260), 260ra148 (2014).
15. Bergholt M. S. et al. *In vivo* diagnosis of esophageal cancer using image-guided Raman endoscopy and biomolecular modeling. *Technol. Cancer Res. Treat.* **10**(2), 103-112 (2011).

16. Bergholt M.S. et al. Raman endoscopy for objective diagnosis of early cancer in the gastrointestinal system. *J. Gastroint. Dig. Syst.* 01 (2013).

17. Wang, J. et al. Comparative study of the endoscope-based bevelled and volume fiber-optic Raman probes for optical diagnosis of gastric dysplasia *in vivo* at endoscopy. *Anal. Bioanal. Chem.* **407**, 8303-8310 (2015).

18. Riccardo C. et al. Combined fluorescence-Raman spectroscopic setup for the diagnosis of melanocytic lesions. *J. Biophotonics.* **7**, 86-95 (2014).

19. Zavaleta C.L. et al. A Raman-based endoscopic strategy for multiplexed molecular imaging. *Proc. Natl. Acad. Sci.* **110**, E2288-2297 (2013).

20. Jeong S. et al. Fluorescence-Raman dual modal endoscopic system for multiplexed molecular diagnostics. *Sci. Rep.* **5**, 9455 (2015).

21. Kim Y. et al. Simultaneous detection of EGFR and VEGF in colorectal cancer using fluorescence-Raman endoscopy. *Sci. Rep.* **7**, 1035 (2017).

22. Woo M. A. et al. Multiplex immunoassay using fluorescent-surface enhanced Raman spectroscopic dots for the detection of bronchioalveolar stem cells in murine lung. *Anal. Chem.* **81**(3), 1008-1015 (2009).

23. Wang Y. W. et al. *In vivo* multiplexed molecular imaging of esophageal cancer via spectral endoscopy of topically applied SERS nanoparticles. *J. Biomed. Opt.* **6**(10), 3714-3723 (2015).

24. Stöber W. et al. Controlled growth of monodisperse silica spheres in the micron size range. *J. Colloid Interface Sci.* **26**, 62-69 (1968).

국문 초록

근래들어 암의 조기 진단에 대한 수요 및 필요성 증가와 광학적 기술 증대라는 두 조건이 맞물려 내시경 기술에 분광학적 분석 기능이 추가된 진단 장비들이 활발하게 개발되고 있다. 이러한 장비들은 생체 조직에 내재된 신호를 기반으로 분석하는 비표지 분석법을 이용한 장비와 특정 생체 마커에 특이적으로 결합하는 표지자를 사용하는 표지 분석법을 이용한 장비로 나뉘는데, 이 같은 기술은 기존에 백색광 내시경 영상 기술을 통하여 발견하지 못했던 병변에 대한 진단을 가능케하고있다. 하지만 현재 이용되고 있는 형광 기반의 표지자의 경우 그 선폭이 넓고 생체 조직이 발하는 자가형광과의 겹침 가능성이 있다는 한계가 존재한다. 이에 최근 연구들에서는 좁은 선폭과 높은 민감도를 지닌 표면증강라만산란(surface enhanced Raman scattering, SERS) 나노 입자를 표지자로 사용하여 내시경 기반 다중 진단에 활용하려는 시도가 이어지고 있다.

본 연구에서는 기 개발된 형광-라만 동시 측정 내시경 장비에서 활용할 수 있는 형광-표면 증강 라만 산란 신호를 동시에 내면서 서로 신호 간섭 없이 분리할 수 있는 나노 프로브(F-SERS dot)를 합성하여 광학적안정성을 검증하였다. 또한 F-SERS dot 을 암 특이 생체 마커에 대한 표지자로 활용하기 위하여 입자 표면에 항체를 EDC/NHS 결합법으로 고정하였다. 합성한 나노 프로브의 특이적 검출 가능성을 검증하기 위하여

직장암 모델에서의 종양 세포 생체 마커로서 표피생장인자 수용체(epidermal growth factor receptor, EGFR)와 혈관내피성장인자(vascular endothelial growth factor, VEFG)를 택하여 이에 대한 항체를 각기 다른 라만 신호 분자가 표지된 F-SERS dot 에 고정함으로써 종양 세포에 대한 다중 검출을 수행하였다.

주요어 : 형광-라만 나노프로브(F-SERS dot), 표면 증강 라만 산란 (SERS), 형광-라만 동시 측정 내시경 시스템, 직장암, 체내 다중 분자 진단

학번 : 2015-23061